ISSN: 2150-4091 Volume 6, Number 17, December 2014

Scientific Research

Natural Science

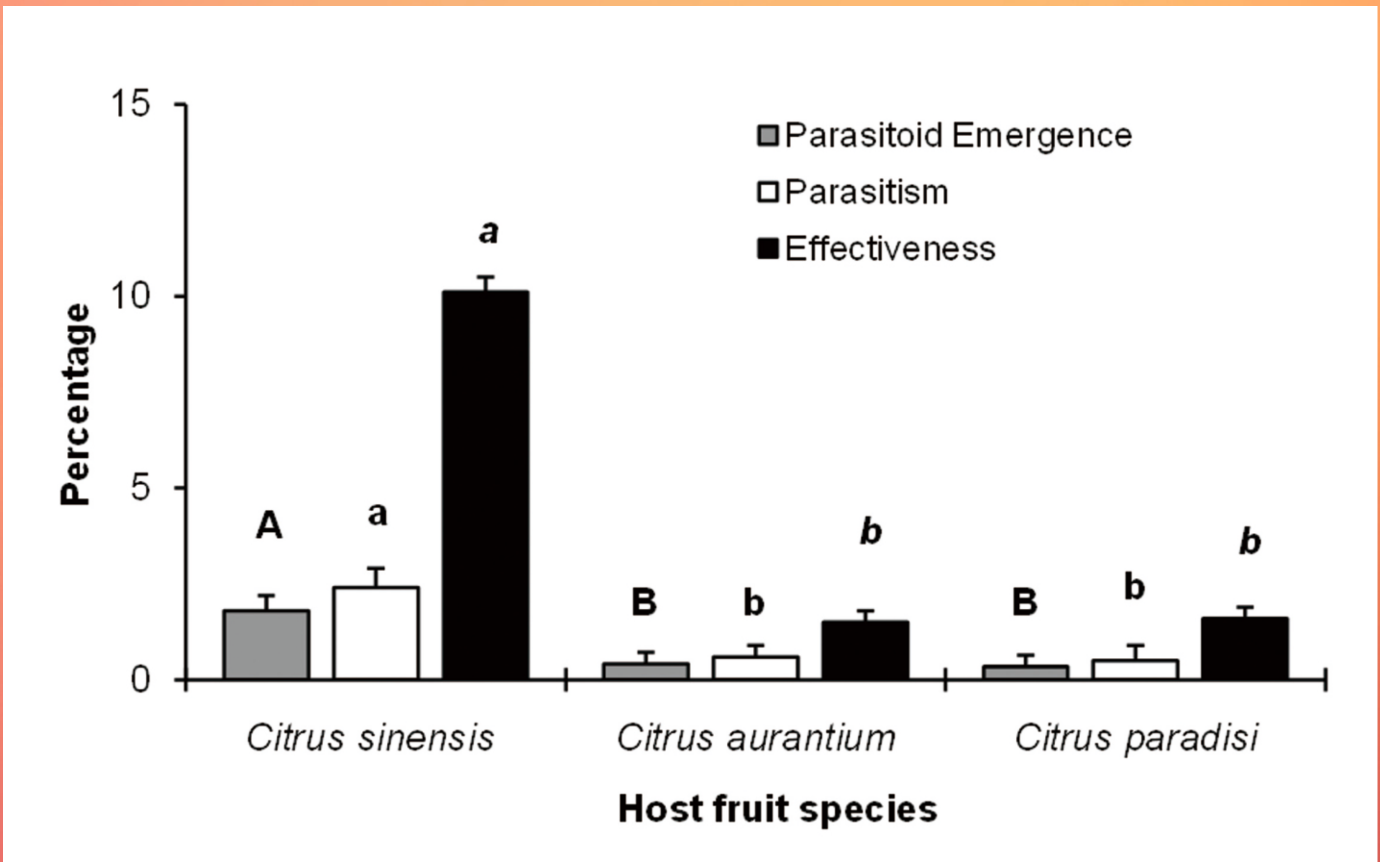

ISSN: 2150-4091

Editor-in-Chief
Kuo-Chen Chou

www.scirp.org/journal/ns

Journal Editorial Board

ISSN: 2150-4091 (Print) ISSN: 2150-4105 (Online)
http://www.scirp.org/journal/ns

Natural Science, 2014, 6, 1267-1295
Published Online December 2014 in SciRes. http://www.scirp.org/journal/ns

Table of Contents

Volume 6 Number 17 December 2014

The figure on the front cover is from the article published in Natural Science, 2014, Vol. 6, No. 17, pp. 1267-1274 by Patricia Albornoz Medina, *et al.*

Natural Science (NS)

Journal Information

SUBSCRIPTIONS

The *Natural Science* (Online at Scientific Research Publishing, www.SciRP.org) is published monthly by Scientific Research Publishing, Inc., USA.

Subscription rates:

Print: $89 per copy.
To subscribe, please contact Journals Subscriptions Department, E-mail: sub@scirp.org

SERVICES

Advertisements
Advertisement Sales Department, E-mail: service@scirp.org

Reprints (minimum quantity 100 copies)
Reprints Co-ordinator,Scientific Research Publishing, Inc., USA.
E-mail:sub@scirp.org

COPYRIGHT

PRODUCTION INFORMATION

For manuscripts that have been accepted for publication, please contact:
E-mail: ns@scirp.org

Natural Science, 2014, 6, 1267-1274
Published Online December 2014 in SciRes. http://www.scirp.org/journal/ns
http://dx.doi.org/10.4236/ns.2014.617116

Mortality by Parasitization in the Association between *Diachasmimorpha tryoni* (Hymenoptera: Braconidae) and *Ceratitis capitata* (Diptera: Tephritidae) under Field-Cage Conditions

Patricia Albornoz Medina, Guido Van Nieuwenhove, Laura Patricia Bezdjian, Pablo Schliserman, Claudia Fidelis-Marinho, Sergio Marcelo Ovruski*

Laboratorio de Investigaciones Ecoetológicas de Moscas de la Fruta y sus Enemigos Naturales (LIEMEN), División Control Biológico de Plagas, Planta Piloto de Procesos Industriales Microbiológicos y Biotecnología (PROIMI)—CCT Tucumán—CONICET, Tucumán, Argentina
Email: palbornozmedina@gmail.com, gavn12004@yahoo.com.ar, laurabezdjian@yahoo.com.ar, cfmarinhoo@gmail.com, schliserman73@yahoo.com.ar, *ovruskisergio@yahoo.com.ar

Received 18 October 2014; revised 12 November 2014; accepted 28 November 2014

Abstract

***Ceratitis capitata* (Wiedemann) is one of the major pests currently affecting world fruit production. In Argentina's northern *Citrus*-producing regions, *C. capitata* is actively multiplying in large exotic host fruits, such as *Citrus paradisi* Macfadyen (grapefruit), *Citrus aurantium* L. (sour orange) and *Citrus sinensis* L. (Osbeck) (sweet orange). Faced with this situation, the use of parasitoids as bio-control agents is currently receiving renewed attention as a new biological tool for controlling pestiferous fruit flies within the Argentinean National Fruit Fly Control and Eradication Program (ProCEM). Consequently, a viable approach to controlling *C. capitata* involves the use of exotic parasitoids such as *Diachasmimorpha tryoni* (Cameron). In this study, the effectiveness of *D. tryoni* females to find and successfully parasitize *C. capitata* larvae infesting all *Citrus* species mentioned earlier was assessed. Parasitoids were allowed to forage for 8 h on grapefruits and oranges artificially infested with laboratory-reared *C. capitata* larvae under natural environmental conditions (field cage). Parasitoid emergence, parasitism, overall effectiveness, and sex ratio of parasitoid offspring were estimated as response variables. The higher effectiveness of *D. tryoni* females recorded from *C. sinensis* would be mainly a result of both increased host density per unit of fruit surface area and fruit physical features. The study provides evidence that *D. tryoni* contributed to**

*Corresponding author.

How to cite this paper: Medina, P.A., Van Nieuwenhove, G., Bezdjian, L.P., Schliserman, P., Fidelis-Marinho, C. and Ovruski, S.M. (2014) Mortality by Parasitization in the Association between *Diachasmimorpha tryoni* (Hymenoptera: Braconidae) and *Ceratitis capitata* (Diptera: Tephritidae) under Field-Cage Conditions. *Natural Science*, **6**, 1267-1274.
http://dx.doi.org/10.4236/ns.2014.617116

***C. capitata* mortality in all *Citrus* species assessed. However, the mortality values recorded from *C. sinensis*, *C. aurantium*, and *C. paradisi* did not exceed 10%, 1.5%, and 1.7%, respectively. Nonetheless, *D. tryoni* might be selected to forage under both high and low host density conditions.**

Keywords

Fruit Fly, *Citrus*, Parasitoid, Biological Control, Argentina

1. Introduction

The Mediterranean fruit fly (Medfly), *Ceratitis capitata* (Wiedemann), is one of the major pests of commercial fruit crops in Argentina. This tephritid species is widely distributed throughout Argentina, and severely limit the export of fresh fruit as a result of quarantine restrictions in countries free of this pest [1]. In Argentina's northern *Citrus*-producing regions, *C. capitata* is actively multiplying in large exotic host fruits, such as *Citrus paradisi* Macfadyen (grapefruit), *Citrus aurantium* L. (sour orange) and *Citrus sinensis* L. (Osbeck) (sweet orange) (Rutaceae), all originated in Southeast Asia [2]. These *Citrus* species are commonly found in abandoned crop fields or in disturbed wild vegetation areas [3].

In Argentina, there is an increasing interest in combating *C. capitata* through ecologically acceptable practices, including both the use of natural enemies and the sterile insect technique, aimed towards the conservation of biodiversity in agroecosystems [1] [4]. Fortunately, the use of hymenopterous parasitoids as biocontrol agents is currently receiving renewed attention as a new biological tool for controlling pestiferous fruit flies within the Argentinean National Fruit Fly Control and Eradication Program (ProCEM) [5]. The most recent introduction of parasitoids in Argentina for fruit fly biological control took place in 1999. Two Indo-Pacific parasitoid species, *Diachasmimorpha longicaudata* (Ashmead) and *D. tryoni* (Cameron), were introduced in Argentina via Mexico for augmentative releases against *C. capitata* [6]. Both braconid species are solitary, koinobiont endoparasitoids, which attack late instar larvae of several fruit-infesting tephritid flies [7]. However, only *D. longicaudata* is currently being mass-reared at the "BioPlanta San Juan" facility from ProCEM-San Juan [4], and it is also being massively released against *C. capitata* in several fruit-producing valleys in the province of San Juan [8]. Although *D. tryoni* was successfully colonized at the laboratory on larvae of *C. capitata*, it was reared on a small scale and was not released [6].

Diachasmimorpha tryoni has been used in classical and augmentative biological control programs in Central America and Hawaii against tephritid pests such as *Ceratitis capitata* (Wiedemann), *Anastrapha suspensa* Loew, *A. obliqua* (Macquart), and *Bactrocera dorsalis* (Hendel) [7] [9]-[14]. In Hawaii, augmentative releases of *D. tryoni* against *C. capitata* showed that overall parasitism rates were increased by 48% [15]-[17]. In Guatemala, aerial mass-releases of *D. tryoni* into coffee crops affected by *C. capitata* achieved parasitism levels close to 84% [11].

Large exotic fruits highly infested by *C. capitata* larvae in northern Argentinian fruit-producing areas, such as *Citrus* spp., represent a vacant niche which could be exploited by exotic parasitoid species with suitable individual abilities to successfully attack the Mediterranean fruit fly [2]. Consequently, the prediction that females of *D. tryoni* would be most efficient in suppressing *C. capitata* larvae infesting *C. paradisi*, *C. aurantium* and *C. sinensis* fruits was assessed. This prediction was based on the good capacity of *D. tryoni* for successful development on the larvae of *C. capitata* [10] [17] and on its good performance in lowering Medfly populations in both Hawaii [15] [16] and Guatemala [11] by means of augmentative releases. Therefore, the purpose of this study was to assess the effectiveness of laboratory-reared *D. tryoni* females so as to find and successfully parasitize *C. capitata* larvae depending on the *Citrus* species under natural conditions. This research is part of a series of studies evaluating the efficacy of several exotic and native parasitoid species to kill *C. capitata* larvae infesting *Citrus* species in Argentina [2] [5].

2. Material and Methods

2.1. Importation of Parasitoid

The parasitoid *D. tryoni* was obtained from a colony that had been maintained on larvae of *C. capitata* at the Biological Control Laboratory of Mexico's Moscamed-Moscafrut National Program and imported to Argentina within irradiated *C. capitata* pupae in 1999 [6]. The shipment was immediately brought to the quarantine facility at the Research Center for the Control of Harmful Organism Populations (CIRPON) in San Miguel de Tucumán, Argentina. Several generations later, the *D. tryoni* colony was transferred to the Ecological Research Laboratory of Fruit Flies and their Natural Enemies (LIEMEN) from the Biological Control Division of the Pilot Plant of Industrial Microbiological Processes and Biotechnology (PROIMI) in San Miguel de Tucumán.

2.2. General Insect Rearing Conditions

The parasitoid *D. tryoni* was reared on third-instar larvae of a wild *C. capitata* strain in the LIEMEN at PROIMI institute. Adult parasitoids were kept in cubical plexiglas cages (30 cm) holding 500 pairs per cage at 25˚C ± 1˚C; 75% ± 5% RH and a photoperiod of 12:12 (L:D). Parasitoids were daily provided with honey, soaked in paper towels on the top of a Petri dish, and with a small glass that held wet cotton. Every day, each cage was provided with one oviposition unit composed of an organdy screen-covered dish (10 cm diametre and 1 cm deep) containing about 750 host larvae. This unit was placed inside of the cage. After exposure to the parasitoids, each oviposition unit was removed from the cages. Parasitized *C. capitata* larvae were then placed in emergence cups (50 cm diametre, 65 cm deep) with mesh-screen covers and containing sterilised Vermiculite® as the pupation medium on the bottom. The cups were kept under the above mentioned laboratory conditions until the emergence of adult parasitoids or flies. The larvae of wild *C. capitata* strain were also reared at LIEMEN on wheat germen-based diet fortified with brewer's yeast, sugar, agar-agar, citric acid, sodium benzoate, nipagin and water.

2.3. Field-Cage Test

The assay was carried out to assess the capability of *D. tryoni* in parasitising *C. capitata* larvae infesting three different species of *Citrus*, such as *C. paradisi* ("March" cultivar), *C. aurantium* (rootstock, wild cultivar), and *C. sinensis* ("tanjarina" cultivar) fruits. The experiment was a multiple-choice test performed under no controlled environmental conditions inside a field-cage at the experimental yard of the Research Centre for Control of Harmful Organisms Populations (CIRPON) in San Miguel de Tucumán, Argentina. The study site is located at 26˚50'S, 65˚13'W, and 426 m above sea level and has a mean annual rainfall of 945 mm and a mean annual temperature of 25.3˚C [2]. The assay was performed on October, and the temperature fluctuated between 19.2 and 31.0˚C (mean 21.9˚C), and the relative humidity fluctuated between 49.7% and 83.2% (mean 63.2%).

Sweet oranges, sour oranges, and grapefruits used in the assay were collected from unsprayed trees grown in backyard gardens located in the outskirts of Tafí Viejo district (Tucumán). Several branches of those *Citrus* trees, each containing 3 - 7 unripe fruits, were covered with a cloth mesh in order to avoid fly infestation. Once the fruit reached maturity, they were harvested and transported to LIEMEN. Overall, 24 similar-size fruit per *Citrus* species were selected and individually weighed, and the rind thickness and pulp depth were measured. The rind thickness was determined by measuring the exocarp and mesocarp, while the pulp depth was determined by measuring the endocarp. In addition, the surface area of each *Citrus* fruit was calculated using the formula: sphere surface area = $4\pi r^2$. Weights and measurements are detailed in **Table 1**.

Each ripe grapefruit or sweet orange or sour orange fruit was artificially infested by removing its pulp and replacing it with 120 laboratory-reared third-instar *C. capitata* [2]. Later, inoculated *Citrus* fruits were transported to CIRPON. In this place, experiment was conducted inside a cylindrical nylon field cage (2 m diametre, 3 m height) surrounded by willow trees that provided shade. The cage was protected from rain by a translucent fibre glass roof that allowed natural light to go through. The fruits were distributed inside cage using a similar method to that described by [2]. One inoculated fruit of each *Citrus* species was individually hung from the ceiling of

Table 1. Physical characteristics (mean ± SE) of the three tested host *Citrus* species (*C. paradisi*, *C. aurantium* and *C. sinensis*).

Host *Citrus* species	Weight (g)	Rind thickness (cm)	Pulp depth (cm)	Surface area (cm^2)
C. paradisi	432.9 ± 4.7	0.69 ± 0.02	9.03 ± 0.05	276.3 ± 1.7
C. aurantium	330.4 ± 3.3	0.73 ± 0.01	7.56 ± 0.05	231.2 ± 1.9
C. sinensis	96.3 ± 2.1	0.28 ± 0.01	4.32 ± 0.07	133.1 ± 1.4

the field cage and positioned to form a central circle (50 cm diametre) 2 m above ground level. A small potted lemon tree (1 m height) was placed below each test fruit to simulate a natural environment. All of the fruits were equidistant from each other, and their positions were randomised at each replication. Twenty naïve, 5-day-old, mated *D. tryoni* females were released inside the field cage at the central point of the circle formed by the test *Citrus* fruits at 2 m above ground level. Parasitoid females were allowed to forage freely for 8 h starting at 09:00 h. After exposure time to parasitoids, the fruits were removed from the cage. In the laboratory all fruits were dissected to retrieve *C. capitata* larvae, and the number of dead larvae per fruit was recorded. The living larvae were placed into plastic cups (7 cm diameter, 6 cm height) with sterilised Vermiculite® on the bottom as a pupation substrate. The top of each cup was tightly covered with a piece of organdy. The cups were placed in a room at 24˚C - 26˚C and 70‰ - 80‰ RH with a 12:12 (L:D) h regime. The pupae were moistened weekly to avoid desiccation and were held inside the cups until adult flies or parasitoids emerged. After the insect emergence was complete, the non-enclosed puparia were dissected to check for the presence or absence of immature parasitoid stages and/or fully developed pharate-adult parasitoids. The number and sex of the emerged parasitoids and flies, as well as the number of non-enclosed puparia were recorded. Control tests (inoculated fruit not exposed to parasitoids) were also conducted to determine natural *C. capitata* mortality and adult emergence rates. The assay and the control test were replicated 12 times. For each replicate, a new parasitoid cohort was released into the cage, and new inoculated fruits were hung from the cage roof.

2.4. Data Analysis

For data analysis, the dependent variables "parasitoid emergence", "parasitism", "overall effectiveness", and "sex ratio of parasitoid offspring" were estimated. The adult parasitoid emergence was calculated as the number of emerged adult parasitoids divided by the total number of recovered pupae ×100. The parasitism percentage was calculated as the number of emerged adult parasitoids plus the number of unemerged parasitoids divided by the total number of pupae recovered from the test fruit ×100. The Abbot's corrected formula was used to determine the overall effectiveness of the parasitoid species for killing the host [18]. The overall effectiveness involves both parasitism and additional host mortality rates [2]. Sex ratio was estimated as the proportion of female offspring. Pearson Product Moment Correlations ($P = 0.05$) were calculated to determine the degree of association between dependent variables before to compare data through univariate or multivariate General Linear Models (GLM) at $P = 0.05$ [19]. Since the fruit size among *Citrus* species was different, but the host density per fruit species was the same, a rate of "host density/cm^2 of fruit surface" was used as a covariate to assess a possible effect of host density on the four dependent variables above listed. Mean comparisons were analysed by Tukey's Honesty Significant Difference (HSD) test at $P = 0.05$. The proportion data were transformed to arcsine square root before analysis. All untransformed means (±SE) were presented in the text.

3. Results

There were significant correlations between the parasitoid emergence, parasitism, and the effectiveness (**Table 2**). Therefore, these response variables were jointly analyzed using a multivariate analysis.

The multivariate GLM showed significant differences among *Citrus* species regarding the parasitoid emergence, parasitism, and the effectiveness, but covariate was negligible (categorical factor: Wilks' $\lambda = 0.57875$, $F_{4, 62} = 4.87429$, $P = 0.00175$, covariate: Wilks' $\lambda = 0.57875$, $F_{2, 31} = 0.10403$, $P = 0.90150$). Because the multivariate GLM was significant, we then followed with univariate GLMs, and its results are detailed in **Table 3**.

Table 2. Summary of Pearson Product Moment Correlations calculated to determine the degree of association between dependent variables (parasitoid emergence, parasitism, effectiveness, and sex ratio of parasitoid offspring).

	Sample size	Parasitoid Emergence	Parasitism	Effectiveness
Parasitoid emergence	$N = 36$	-	$r = 1.00$, $P < 0.001$[a]	$r = 0.47$, $P = 0.003$[a]
Parasitism	$N = 36$	-	-	$r = 0.48$, $P = 0.003$[a]
Effectiveness	$N = 36$	-	-	-
Sex ratio	$N = 36$	$r = 0.34$, $P = 0.132$	$r = 0.35$, $P = 0.131$	$r = 0.25$, $P = 0.127$

[a]Significant variables.

Table 3. Summary of univariate one-way ANOVAs on the *Diachasmimorpha tryoni* females performance in killing *Ceratitis capitata* larvae infesting *Citrus paradisi*, *C. aurantium* and *C. sinensis* fruits (dependent variables: parasitoid emergence, parasitism, effectiveness).

Source of variation	*df*/Error *df*	Parasitoid Emergence	Parasitism	Effectiveness
Host density/cm^2 (covariate)	1, 32	$F = 0.001$, $P = 0.965$	$F = 0.001$, $P = 0.965$	$F = 0.002$, $P = 0.652$
Citrus species (categorical factor)	2, 32	$F = 7.261$, $P = 0.002^a$	$F = 7.261$, $P = 0.002^a$	$F = 4.172$, $P = 0.024^a$

[a]Significant variables.

The percentage of adult parasitoids emerged from *C. capitata* pupae obtained from sweet orange was 3.7- and 5.0-times higher than those recorded from grapefruit and sour orange, respectively (**Figure 1**). Similarly, both the percentage of parasitism and the effectiveness on *C. capitata* were also the highest in sweet orange. Both the parasitism and effectiveness recorded from *C. sinensis* were 3.4- and 3.9-times and 5.7- and 5.4-times higher than those found in both sour orange and grapefruit, respectively (**Figure 1**). There was no significant difference between sour orange and grapefruit regarding the parasitoid emergence, parasitism, and the effectiveness (**Figure 1**). Furthermore, *D. tryoni* exhibited a male-biased sex ratio. The univariate GLM revealed no significant difference in female offspring recovered from the three *Citrus* species (categorical factor: $F_{2, 32} = 2.6325$, $P = 0.0874$, covariate: $F_{1, 32} = 0.9689$, $P = 0.3323$) (**Figure 2**).

4. Discussion

The field cage experiment yielded interesting results, showing that *D. tryoni* females had a better performance in killing *C. capitata* larvae infesting *C. sinensis* than in both *C. paradisi* and *C. aurantium*. Moreover, the effectiveness of *D. tryoni* females on *C. capitata* larvae infesting *C. aurantium* was similar to that recorded from *C. paradisi*. The relatively poor performance of *D. tryoni* at *C. paradisi* and *C. aurantium* appears to support the hypothesis that tephritid larvae infesting larger fruits containing a deep pulp could be more protected from parasitoid attack [20]-[22]. From all *Citrus* species tested in this study, *C. sinensis* had more advantageous physical characteristics to ease parasitoid success, such as a thinner rind and a shallower pulp. As previously suggested for *D. longicaudata* [2] [23]-[25], latter two physical features may have helped *D. tryoni* females better distinguish the vibrations and/or sound caused by *C. capitata* larvae [26] once the parasitoids landed onto the *C. sinensis* fruit. However, other factor such as host density may also have influenced the effectiveness by *D. tryoni*. For instance, *C. sinensis* had the greater number of *C. capitata* larvae per unit of fruit surface area of all *Citrus* species tested (0.90, 0.52, and 0.43 larva/cm^2 in *C. sinensis*, *C. aurantium*, and *C. paradisi*, respectively). This suggests a higher number of host larvae exposed to *D. tryoni* females in *C. sinensis* than in both *C. paradisi* and *C. aurantium*. Even though, quite low effectiveness levels were recorded from *C. capitata* in both *C. paradisi* and *C. aurantium*, it is significant to highlight the fact that *D. tryoni* females were particularly efficient at finding and attacking larvae at low host densities. This result was consistent with published data of *D. tryoni* attacking *Anastrepha ludens* (Loew) in artificially infested guavas into a field cage at canopy level [12].

The same effectiveness pattern recorded for *D. tryoni* in the present study was also found for *D. longicaudata* attacking *C. capitata* larvae in all three aforementioned *Citrus* species [2]. Nevertheless, *D. tryoni* females performed worse than *D. longicaudata* females under natural environmental conditions. For instance, the overall mortality recorded from *C. capitata* inflicted by *D. longicaudata* in *C. paradisi*, *C. aurantium*, and in *C. sinensis* [2] was about 5, 3, and 2 times, respectively, higher than those induced by *D. tryoni*. In contrast, both *D. tryoni* and *D. longicaudata* achieved the highest parasitism rates and also had a similar performance to search, locate and attack *A. ludens* larvae at canopy level in guava trees [12]. This contrasting information will be useful in planned future comparisons between *D. tryoni* and *D. longicaudata* to assess the performance of these two exotic braconid species into low and high host-density environments.

The foraging ecology of parasitoids has implications for pestiferous fruit fly biorational management programmes [27]. Augmentative releases of parasitoids may be mostly successful when combined with the Sterile Insect Technique [14] [16] [28]. A low-density forager, such as *D. tryoni*, might be a convenient candidate for releases because it might continue producing mortality at low host densities [12] [25].

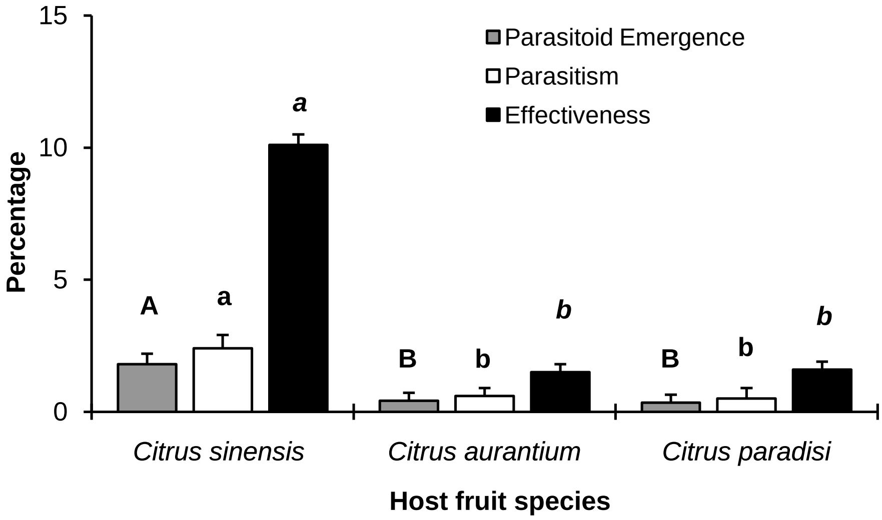

Figure 1. Mean (±SE) percentage of emerged parasitoids, percent parasitism, and effectiveness recorded from artificially infested *C. sinensis*, *C. aurantium* and *C. paradisi* fruits with third-instar *C. capitata* larvae that were parasitised by *D. tryoni* females under natural environmental conditions inside a field cage. Bars followed by the same letter indicate no significant differences (Tukey HSD test, $P = 0.05$).

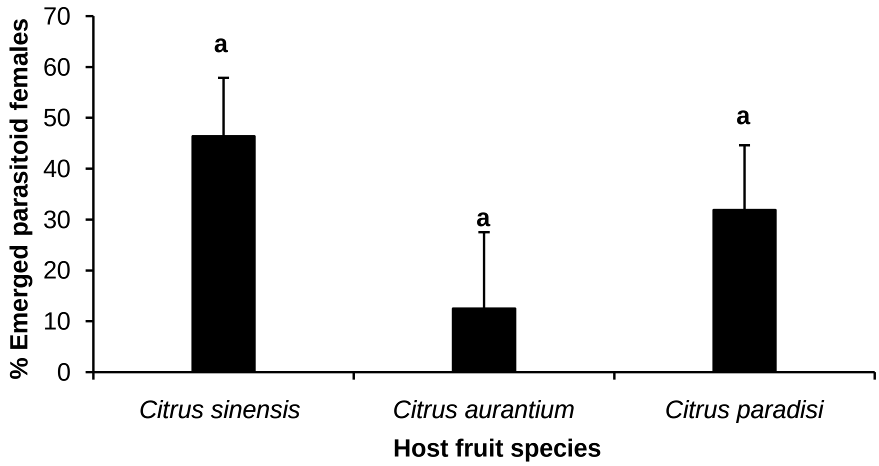

Figure 2. Mean (±SE) percentage of female offspring (sex ratio) recorded from artificially infested *C. sinensis*, *C. aurantium* and *C. paradisi* fruits with third-instar *C. capitata* larvae that were parasitised by *D. tryoni* females under natural environmental conditions inside a field cage. Bars followed by the same letter indicate no significant differences (Tukey HSD test, $P = 0.05$).

5. Conclusions

The study provides evidence that *D. tryoni* contributed to *C. capitata* mortality in all *Citrus* species assessed. However, the mortality values recorded from *C. sinensis*, *C. aurantium*, and *C. paradisi* did not exceed 10%, 1.5%, and 1.7%, respectively. Interestingly, *D. tryoni* might be selected to forage under both high and low host density conditions.

The findings from this study may serve as a preliminary basis for assessing the potential impact of *D. tryoni* on *C. capitata* in *Citrus* species. In future studies, evaluating other major *C. capitata* host plant species found in the fruit-growing areas of northern Argentina, such as peach, plum, fig, and walnut, would help accomplish deeper insight into the performance of *D. tryoni* females in lowering natural populations of *C. capitata* occurring in this Argentinean region.

Acknowledgements

Financial support was provided by the Agencia Nacional de Promoción Científica y Tecnológica de Argentina (ANPCyT) through Fondo Nacional de Ciencia y Tecnología (FONCyT) (grant PICT/2010 No. 0393).

References

[1] Guillén, D. and Sánchez, R. (2007) Expansion of the National Fruit Fly Control Programme in Argentina. In: Vreysen, M.J.B., Robinson, A.S. and Hendrichs, J., Eds., *Area-Wide Control of Insects Pests*: *From Research to Field Implementation*, Springer, Dordrecht, 653-660. http://dx.doi.org/10.1007/978-1-4020-6059-5_60

[2] Ovruski, S.M., Van Nieuwenhove, G.A., Bezdjian, L.P., Albornoz-Medina, P. and Schliserman, P. (2012) Evaluation of *Diachasmimorpha longicaudata* (Hymenoptera: Braconidae) as a Mortality Factor of *Ceratitis capitata* (Diptera: Tephritidae) Infesting *Citrus* Species under Laboratory and Field-Cage Conditions. *Biocontrol Science and Technology*, **22**, 187-202. http://dx.doi.org/10.1080/09583157.2011.648167

[3] Ovruski, S.M., Schliserman, P. and Aluja, M. (2003) Native and Introduced Host Plants of *Anastrepha fraterculus* and *Ceratitis capitata* (Diptera: Tephritidae) in Northwestern Argentina. *Journal of Economic Entomology*, **96**, 1108-1118. http://dx.doi.org/10.1603/0022-0493-96.4.1108

[4] Suárez, L., Van Nieuwenhove, G.A., Murúa, F.A., Bezdjian, L.P., Schliserman, P., Lara, N., Escobar, J. and Ovruski, S.M. (2012) Offspring Production in Response to Host Exposure Times in *Diachasmimorpha longicaudata* (Hymenoptera: Braconidae), Reared on the Genetic Sexing Strain Vienna 8 of *Ceratitis capitata* (Diptera: Tephritidae). *Florida Entomologist*, **95**, 991-999. http://dx.doi.org/10.1653/024.095.0426

[5] Ovruski, S.M. and Schliserman, P. (2012) Biological Control of Tephritid Fruit Flies in Argentina: Historical Review, Current Status, and Future Trends for Developing a Parasitoid Mass-Release Program. *Insects*, **3**, 870-888. http://dx.doi.org/10.3390/insects3030870

[6] Ovruski, S.M., Colin, C., Soria, A., Oroño, L. and Schliserman, P. (2003) Introducción y establecimiento en laboratorio de *Diachasmimorpha tryoni* y *Diachasmimorpha longicaudata* (Hymenoptera: Braconidae, Opiinae) para el control biológico de *Ceratitis capitata* (Diptera: Tephritidae, Dacinae) en la Argentina. *Revista Sociedad Entomológica Argentina*, **62**, 49-59.

[7] Ovruski, S.M., Aluja, M., Sivinski, J. and Wharton, R.A. (2000) Hymenopteran Parasitoids on Fruit-Infesting Tephritidae (Diptera) in Latin America and the Southern United States: Diversity, Distribution, Taxonomic Status and Their Use in Fruit Fly Biological Control. *Integrated Pest Management Reviews*, **5**, 81-107. http://dx.doi.org/10.1023/A:1009652431251

[8] Suárez, L., Murúa, F.A., Lara, N., Escobar, J., Taret, G., Rubio, J.L., Van Nieuwenhove, G.A., Bezdjian, L.P., Schliserman, P. and Ovruski, S.M. (2014) Biological Control of *Ceratitis capitata* (Diptera: Tephritidae) in Argentina: Releases of *Diachasmimorpha longicaudata* (Hymenoptera: Braconidae) in Fruit-Producing Semi-Arid Areas of San Juan. *Natural Science*, **6**, 664-675. http://dx.doi.org/10.4236/ns.2014.69066

[9] Wharton, R.A. (1989) Classical Biological Control of Fruit-Infesting Tephritidae. In: Robinson, A.S. and Hooper, G., Eds., *World Crop Pests*. *Fruit Flies*, *Their Biology*, *Natural Enemies and Control*, Vol. 3B, Elsevier Science, Amsterdam, 303-313.

[10] Purcell, M.F. (1998) Contribution of Biological Control to Integrated Pest Management of Tephritid Fruit Flies in the Tropics and Subtropics. *Integrated Pest Management Reviews*, **3**, 63-83. http://dx.doi.org/10.1023/A:1009647429498

[11] Sivinski, J., Jeronimo, F. and Holler, T. (2000) Development of Aerial Releases of *Diachasmimorpha tryoni* (Cameron) (Hymenoptera: Braconidae), a Parasitoid That Attacks the Mediterranean Fruit Fly, *Ceratitis capitata* (Weidemann) (Diptera: Tephritidae), in the Guatemalan Highlands. *Biocontrol Science and Technology*, **10**, 15-25. http://dx.doi.org/10.1080/09583150029341

[12] García-Medel, D., Sivinski, J., Díaz-Fleischer, F., Ramirez-Romero, R. and Aluja, M. (2007) Foraging Behavior by Six Fruit Fly Parasitoids (Hymenoptera: Braconidae) Released as Single- or Multiple-Species Cohorts in Field Cages: Influence of Fruit Location and Host Density. *Biological Control*, **43**, 12-22. http://dx.doi.org/10.1016/j.biocontrol.2007.06.008

[13] Montoya, P., Cancino, J. and Ruiz, L. (2012) Packing of Fruit Fly Parasitoids for Augmentative Releases. *Insects*, **3**, 889-899. http://dx.doi.org/10.3390/insects3030889

[14] Vargas, R.I., Leblanc, L., Harris, E.J. and Manoukis, N.C. (2012) Regional Suppression of *Bactrocera* Fruit Flies (Diptera: Tephritidae) in the Pacific through Biological Control and Prospects for Future Introductions into Other Areas of the World. *Insects*, **3**, 727-742. http://dx.doi.org/10.3390/insects3030727

[15] Wong, T.T.Y., Ramadan, M.M., McInnis, D.O., Mochizuki, N., Nishimoto, J.I. and Herr, J.C. (1991) Augmentative Releases of *Diachasmimorpha tryoni* (Hymenoptera: Braconidae) to Suppress a Mediterranean Fruit Fly (Diptera: Tephritidae) Population in Kula Maui, Hawaii. *Biological Control*, **1**, 2-7.

http://dx.doi.org/10.1016/1049-9644(91)90094-G

[16] Wong, T.T.Y., Ramadan, M.M., Herr, J.C. and McInnis, D.O. (1992) Suppression of a Mediterranean Fruit Fly (Diptera: Tephritidae) Population with Concurrent Parasitoid and Sterile Fly Release in Kula Maui. *Journal of Economical Entomology*, **85**, 1671-1681.

[17] Vargas, R.I., Ramadan, M., Hussain, T., Mochizuki, N., Bautista, R.C. and Strak, J.D. (2002) Comparative Demography of Six Fruit Fly (Diptera: Tephritidae) Parasitoids (Hymenoptera: Braconidae). *Biological Control*, **25**, 30-40. http://dx.doi.org/10.1016/S1049-9644(02)00046-4

[18] Rosenheim, J.A. and Hoy, M.A. (1989) Confidence Intervals for the Abbott's Formula Correction of Bioassay Data for Control Response. *Journal of Economical Entomology*, **82**, 331-335.

[19] Zar, J.H. (1999) Biostatistical Analysis. Prentice Hall, Upper Saddle River.

[20] Wong, T.T.Y. and Ramadan, M.M. (1987) Parasitization of the Mediterranean and Oriental Fruit Flies (Diptera: Tephritidae) in the Kula Area of Maui, Hawaii. *Journal of Economic Entomology*, **80**, 77-80.

[21] Wang, X.-G., Johnson, M.W., Daane, K.M. and Yokoyama, V.Y. (2009) Larger Olive Fruit Size Reduces the Efficiency of *Psyttalia concolor* as a Parasitoid of the Olive Fruit Fly. *Biological Control*, **49**, 45-51. http://dx.doi.org/10.1016/j.biocontrol.2009.01.004

[22] Wang, X., Nadel, H., Johnson, M.W., Daane, K.M., Hoelmer, K., Pickett, C.H. and Sime, K.R. (2009) Crop Domestication Relaxes Both Top-Down and Bottom-Up Effects on a Specialist Herbivore. *Basic and Applied Ecology*, **10**, 216-227. http://dx.doi.org/10.1016/j.baae.2008.06.003

[23] Leyva, J.L., Browning, H.W. and Gilstrap, F.E. (1991) Effect of Host Fruit Species, Size, and Color on Parasitization of *Anastrepha ludens* (Diptera: Tephritidae) by *Diachasmimorpha longicaudata* (Hymenoptera: Braconidae). *Environmental Entomology*, **20**, 1470-1474.

[24] Sivinski, J., Vulinec, K. and Aluja, M. (2001) Ovipositor Length in a Guild of Parasitoids (Hymenoptera: Braconidae) Attacking *Anastrepha* spp. Fruit Flies (Diptera: Tephritidae) in Southern Mexico. *Annals of the Entomological Society of America*, **94**, 886-895. http://dx.doi.org/10.1603/0013-8746(2001)094[0886:OLIAGO]2.0.CO;2

[25] Sivinski, J. and Aluja, M. (2003) The Evolution of Ovipositor Length in the Parasitic Hymenoptera and the Search for Predictability in Biological Control. *Florida Entomologist*, **86**, 143-150. http://dx.doi.org/10.1653/0015-4040(2003)086[0143:TEOOLI]2.0.CO;2

[26] Duan, J.J. and Messing, R.H. (2000) Effects of Host Substrate and Vibration Cues on Ovipositor-Probing Behavior in Two Larval Parasitoids of Tephritid Fruit Flies. *Journal of Insect Behavior*, **13**, 175-186. http://dx.doi.org/10.1023/A:1007780029320

[27] Aluja, M. and Rull, J. (2009) Managing Pestiferous Fruit Flies (Diptera: Tephritidae) through Environmental Manipulation. In: Aluja, M., Leskey, T.C. and Vincent, C., Eds., *Biorational Tree Fruit Pest Management*, CABI, Oxford, 171-213. http://dx.doi.org/10.1079/9781845934842.0171

[28] Rendón, P., Sivinski, J., Holler, T., Bloem, K., López, M., Martínez, A. and Aluja, M. (2006) The Effects of Sterile Males and Two Braconid Parasitoids, *Fopius arisanus* (Sonan) and *Diachasmimorpha krausii* (Fullaway) (Hymenoptera), on Caged Populations of Mediterranean Fruit Flies, *Ceratitis capitata* (Wied.) (Diptera: Tephritidae) at Various Sites in Guatemala. *Biological Control*, **36**, 224-231. http://dx.doi.org/10.1016/j.biocontrol.2005.10.006

Natural Science, 2014, 6, 1275-1281
Published Online December 2014 in SciRes. http://www.scirp.org/journal/ns
http://dx.doi.org/10.4236/ns.2014.617117

Scientific Research

Deriving of the Generalized Special Relativity (GSR) by Using Mirror Clock and Lorentz Transformations

M. H. M. Hilo[1], R. Abd Elgani[1], R. Abd Elhai[1], M. D. Abd Allah[1], Amel A. A. Elfaki[2]

[1]Department of Physics, Sudan University of Science and Technology, Khartoum, Sudan
[2]Department of Physics, Bahri University, Khartoum, Sudan
Email: mahmoudhilo@gmail.com, mahmoud1972@sustech.edu, rawia_abdalgani@yahoo.com, rawia@sustech.edu, rashaabdelhaye@sustech.edu

Received 1 October 2014; revised 28 October 2014; accepted 15 November 2014

Abstract

Einstein relativity theory shows its high capability of promoting itself to solve the long stand physical problems. The so-called generalized special relativity (GSR) was derived later, using the beautiful Einstein relation between field and space-time curvature. In this work we re-derive (GSR) expression of time by incorporating the field effect in it, and by using mirror clock and Lorentz transformations. This expression reduces to that of (GSR) the previous conventional one, besides reducing to special relativistic expression. It also shows that the speed of light is constant inside the field and is equal to C. This means that the observed decrease of light in matter and field is attributed to the strong interaction of photons with particles and mediates which causes successive absorption and reemission processes that lead to time delay. This absorption process makes some particles appear to move faster than light within the field or medium. This new expression, unlike that of GSR, can describe time and coordinate relativistic expressions for strong as well as weak fields at constant acceleration.

Keywords

Lorentz Transformations, Mirror Clock, Space-Time Curvature, Gravitational Field

1. Introduction

Einstein's special relativity and general relativity represent one of the biggest achievements that change radically the space-time concept [1]. Special relativity (SR) succeeds in explaining the constancy of light speed in va-

How to cite this paper: Hilo, M.H.M., Abd Elgani, R., Abd Elhai, R., Abd Allah, M.D. and Elfaki, A.A.A. (2014) Deriving of the Generalized Special Relativity (GSR) by Using Mirror Clock and Lorentz Transformations. *Natural Science*, **6**, 1275-1281.
http://dx.doi.org/10.4236/ns.2014.617117

cuum, long-time meson decay, and mass-energy conversion [2].

SR shows that time, length, mass, and energy are velocity dependent [3]. Einstein extends his SR theory to the so-called general relativity theory (GR) which extends the space-time interval to the curved space GR succeeded in explaining a wide variety of astronomical phenomena. These include the Doppler red shift, which is interpreted as resulting from the universe expansion, the existence of relic microwave background, beside the gravitational red shift [4].

These remarkable successes of SR and GR motivate some authors to promote SR within the frame of GR to produce the so-called Generalized Special Relativity (GSR) [5].

Mubarak model, the matter energy-momentum tenser relation on the generalized Lorentz factor (r) derived from the space-time interval in the curve space, was utilized to construct the seminal EGSR model; time, length, mass and energy are dependent on the field potential as well as velocity [6].

In this work two mirrors of certain length, acting as time clock, are under the action of gravity. The motion of the two mirrors under gravity is utilized to find a useful expression of time in the presence of the gravitational field. The speed of light is assumed to be constant in the gravity field. This assumption is confirmed by obtaining the light speed in accursed space time [7].

This paper, which is concerned with the derivation of time dilation in the gravitational field, consists of 3 sections; apart from introduction, Section 2 is devoted for presenting EGSR theory. The derivation of time dilation in the gravitational field for any field is done in Section 3. The speed of light in the gravitational field is found in Section 4. Sections 5 and 6 are devoted for discussion and conclusion (Generalized Special Relativity [8]).

According to GSR the expressions of time t, length L, and mass m, are dependent on the velocity as well as field potential per unit mass and according to the relations.

$$t = \frac{t_0}{\sqrt{9_{00} - v^2/c^2}} \tag{1}$$

$$L = L_0\sqrt{9_{00} - v^2/c^2} \tag{2}$$

$$m = \frac{9_{00}\, m_0}{\sqrt{9_{00} - v^2/c^2}} \tag{3}$$

where

$$9_{00} = 1 + \frac{2\phi}{c^2} \tag{4}$$

c stands for light speed in vacuum, while L_0 and m_0 represent the rest time, length and mass respectively.

2. Time Dilation and Length Contraction

The expression of time in the presence of gravitational field can be found by considering two as a clock, with time intervals to representing the travel between the two mirrors as shown in **Figure 1**.

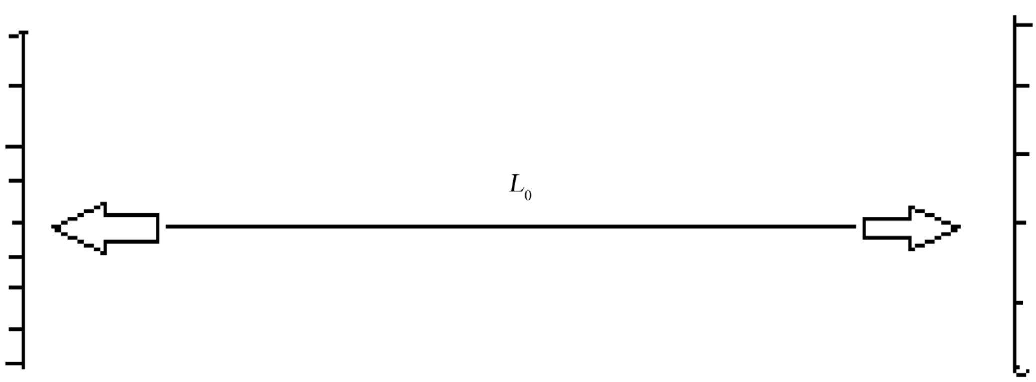

Figure 1. The mirror in free space.

$$L_0 = ct_0 \tag{5}$$

It moves with velocity up ward under gravity of acceleration g, the velocity of the lower mirror is given by

$$v^2 = v_0^2 - 2ay \tag{6}$$

where v_0 stands for the initial velocity, while y represents the displacement.

The vertical displacement y is given by

$$y = v_0 t - \frac{1}{2} a t^2$$

The speed v is also given by $v = v_0 - at$

Thus

$$y = \frac{(2v_0 - at)t}{2} = \frac{(v_0 + v_0 - at)t}{2} = \frac{(v_0 + v)t}{2} = v_a t \tag{7}$$

where: $v_a = \frac{(v_0 + v)}{2}$ →(8) is the average speed; *a* is any arbitrary acceleration in general. For the force F the potential v is given by

$$F = ma, \quad V = may = m\phi$$

where ϕ is the potential per unit mass and is given to be

$$\phi = ay = gy \tag{9}$$

Inserting (9) in (6) yields as shown in **Figure 2**.

$$v^2 = v_0^2 - 2\phi \tag{10}$$

Since the point p at which the photon hits the mirror is displaced y meter vertically down ward, it follows that the light photon hits p as shown in **Figure 3**.

Figure 2. The mirror at $t = 0$.

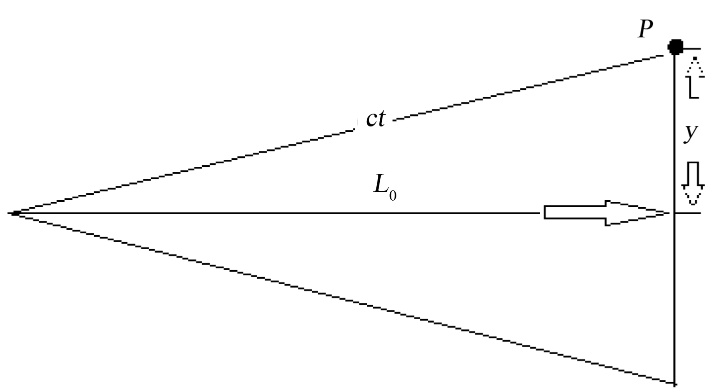

Figure 3. The mirror displaced y meter vertically down ward.

Speed c in the gravitational field the distance travelled by light is given indicates that

$$(ct)^2 = L_0^2 + y^2$$

In view of Equations (7)-(10), one gets

$$c^2t^2 = ct_0^2 + v_m^2 t^2$$

$$\left(1 - \frac{v_m^2}{c^2}\right) t^2 = t_0^2$$

$$t = \frac{t_0}{\sqrt{1 - \frac{v_a^2}{c^2}}} = \frac{t_0}{\sqrt{1 - \frac{(v_0 + v)^2}{4c^2}}} = \gamma t_0 \tag{11}$$

Thus:

$$\gamma = \frac{1}{\sqrt{1 - \frac{v_a^2}{c^2}}} = \frac{1}{\sqrt{1 - \frac{(v_0 + v)^2}{4c^2}}} \tag{12}$$

Using relation (10)

$$\gamma = \frac{1}{\sqrt{1 - \frac{v_0^2 + 2vv_0 + v^2}{4c^2}}},$$

$$\gamma = \frac{1}{\sqrt{1 - \frac{\left(2v_0^2 - 2\phi + 2v_0\sqrt{v_0^2 - 2\phi}\right)}{4c^2}}}. \tag{13}$$

If one consider v and v_0 as standing for effective speed which is related to the maximum speed through the relations

$$v_0 = \frac{1}{\sqrt{2}} v_{0_{\max}}, \quad v = \frac{1}{\sqrt{2}} v_{\max} \tag{14}$$

Then relation (10) becomes

$$v_m^2 = v_{0_{\max}}^2 - 4\phi \tag{15}$$

And relation (13) becomes

$$\gamma = \frac{1}{\sqrt{1 - \frac{\left(2v_{0_{\max}}^2 - 4\phi + 2v_{0_{\max}}\sqrt{v_{0_{\max}}^2 - 4\phi}\right)}{4c^2}}}$$

For weak field

$$2v_0\left(v_{0_{\max}}^2 - 4\phi\right)^{\frac{1}{2}} = 2v_{0_{\max}}^2\left(1 - \frac{4\phi}{v_{0_{\max}}^2}\right)^{\frac{1}{2}} \approx 2v_{0_{\max}}^2 - 4\phi$$

Thus

$$\gamma = \frac{1}{\sqrt{1 - \frac{\left(2v_{0_{\max}}^2 - 4\phi + 2v_{0_{\max}}^2 - 4\phi\right)}{4c^2}}} = \frac{1}{\sqrt{1 + \frac{2\phi}{c^2} - \frac{v_{0_{\max}}^2}{c^2}}} \tag{16}$$

Which coincides completed with the expression of time in the presence of the gravitational field obtain within the framework of GSR. Relation (14) it is important to note that of the factor $1/2$ in Einstein SR energy expression where

$$E = \frac{1}{2} m v_m^2 = m \left(\frac{v_m}{\sqrt{2}} \right)^2 = m v^2 \tag{17}$$

According to Equations (9) and (10) this relation holds for any field other than the gravitational field.

The length contraction can be obtained by considering a clock falling by sliding on a rod of a height L_0. For the observer moving with a clock the average speed is given by

$$v = \frac{L}{t_0} \tag{18}$$

where the rod is moving and accelerated w.r.t him, thus his length is L. But for an observer at rest w.r.t the rod, the rod length is L_0 for him and the clock time is it. Thus the speed v is given by

$$v = \frac{L_0}{t} \tag{19}$$

Thus, with the aid of Equations (18) (19) and (13).

$$\begin{gathered} \frac{L}{t_0} = \frac{L_0}{t} \\ L = L_0 \frac{t_0}{t} = \gamma^{-1} L_0 \end{gathered} \tag{20}$$

This is in agreement with the corresponding expression in GSR.

3. Derivation of Time and Coordinate Expressions by Using Lorentz Transform

Using Lorentz transformation, the event at point (x_1, t_1) in the frame x at a point x is given to be according to Equation (7) by replacing y by x

$$x = \gamma \left(x' + v_a t' \right) \tag{21}$$

Since the space is homogeneous it follows that

$$x' = \gamma \left(x + v_a t \right) \tag{22}$$

Consider ampoule of light emitted from a source when the origins 0 and 01 are in coincidence at

$$t = t' = 0$$

In this care

$$\begin{gathered} x = ct \\ x' = ct' \end{gathered} \tag{23}$$

Substituting Equation (23) in Equations (22) and (21) yields

$$ct = \gamma \left(ct' + v_a t' \right) = \gamma \left(c + v_a \right) t' \tag{24}$$

$$ct' = \gamma \left(ct - v_a t \right) = \gamma \left(c - v_a \right) t \tag{25}$$

Inserting Equation (25) in Equation (24) yields

$$ct = \frac{\gamma^2}{c} \left(c + v_a \right) \left(c - v_a \right) t$$

$$c^2 = \gamma^2 \left(c^2 - v_a^2 \right) t$$

$$\gamma = \frac{1}{\sqrt{1-\frac{v_a^2}{c^2}}} \tag{26}$$

With the aid of Equation (8) and Equation (10)

$$\gamma = \frac{1}{\sqrt{1-\frac{\left(v_0^2+2vv_0+v^2\right)}{4c^2}}} = \frac{1}{\sqrt{1-\frac{\left(v_0^2-\phi+v_0\sqrt{v_0^2-2\phi}\right)}{2c^2}}} \tag{27}$$

When one consider the expression for the maximum speed in Equation (15), one gets

$$\gamma = \frac{1}{\sqrt{1-\frac{\left(v_{0_{\max}}^2-2\phi+v_{0_{\max}}\sqrt{v_{0_{\max}}^2-4\phi}\right)}{2c^2}}} \tag{28}$$

It is very striking to observe that when no field exist, *i.e.* $\phi = 0$

$$\gamma = \frac{1}{\sqrt{1-\frac{v_{0_{\max}}^2}{c^2}}} \tag{29}$$

This is the usual SR expression.
For weak field

$$\frac{\phi}{v_{0_{\max}}^2} \prec\prec 1$$

Therefore

$$\left(v_{0_{\max}}^2-4\phi\right)^{\frac{1}{2}} = v_{0_{\max}}\left(1-\frac{2\phi}{v_{0_{\max}}^2}\right)$$

Thus Equation (25) becomes

$$\gamma = \sqrt{1-\frac{\left(v_{0_{\max}}^2-2\phi+v_{0_{\max}}^2-2\phi\right)}{2c^2}} \tag{30}$$

This is the usual expression of GSR for a weak field.

4. Discussion

In Section 3 time dilation expression in the presence of any field has been derived by using mirror, see Equations (11) and (14). The only assumption which causes a limitation to this expression is the constancy of acceleration. The mirror motion is described by using Newton's Law of linear motion with constant acceleration.

The speed of light is assumed to be constant. The resulting expression for t reduced to that of SR in the absence of a field as shown by Equation (16) where

$$\gamma = \frac{1}{\sqrt{1-\frac{v_{0_{\max}}^2}{c^2}}}$$

It also reduced to GSR form for a weak field as shown in Equation (16).

The expression of length contraction has been obtained as well. Again this expression reduced to SR and GSR also [9].

Lorentz transformation is also utilized to find a relativistic expression for t and x. The expression shown in

Equations (27)-(29) indicates that these expressions are similar to that obtained by the mirror method and are reduced to the corresponding SR and GSR expressions.

5. Conclusion

The expressions for time and length obtained by using Lorentz transformation and using mirror clock, for fields at constant acceleration, and by assuming the speed of light to be constant indicate that GSR rests on a solid ground. It also indicates that space and time are affected by any field, not gravity only. Unlike the curved space-time derivation, where the field is assumed to be week, this derivation holds for strong fields as well. By reducing to SR and GSR for a weak field, it indicates its self-consistency.

References

[1] Lawdre, D.F. (1982) An Introduction to Tensor Calculus and Relativity. John Wiley and Sons, New York, Chapter 5, 6.

[2] Weinberg, S. (1972) Gravitation and Cosmology. John Wiley and Sons, New York, Chapter 5, 6.

[3] Savickas, D. (2002) Relation between Newtonian Mechanics, General Relativity and Quantum Mechanics. *Journal of Physics*, **70**, 798-807.

[4] Mubarak, D.A. and Ali, T. (2003) The Special Relativity in the Presence of Gravitation and Other Field. University of Khartoum, Khartoum.

[5] Dirrar, M., Hilo, M.H.M., Abd Elgani, R. and Bakheet, A.M.A. (2013) Neutrino Speed Can Exceed the Speed of Light within the Frame Work of the Generalized Special Relativity and Savickas Model. *Natural Science*, **5**, 685-688. http://dx.doi.org/10.4236/ns.2013.56084

[6] Hilo, M.H.M. (2011) Using of the Generalized Special Relativity in Deriving the Equation of the Gravitational Red-Shift. *Journal of Modern Physics*, **2**, 370-373. http://dx.doi.org/10.4236/jmp.2011.25045

[7] Hilo, M.H.M., *et al.* (2011) Using of the Generalized Special Relativity (GSR) in Estimating the Neutrino Masses to Explain the Conversion of Electron Neutrinos. *Natural Science*, **3**, 334-338. http://dx.doi.org/10.4236/ns.2011.34044

[8] Narlikar, J.V. (1993) Introduction to Cosmology. 2nd Edition, Cambridge University Press, Cambridge.

[9] Xu, C., Uis, G.F.R.E., Xu, X.J. and El Tahir, A. (1992) The Generalized Field Equation. *South African Journal of Physics*, **15**, 5.7.

Natural Science, 2014, 6, 1282-1285
Published Online December 2014 in SciRes. http://www.scirp.org/journal/ns
http://dx.doi.org/10.4236/ns.2014.617118

Scientific Research

A Form of Information Entropy

M. Divari, D. Vivona

Department of Basic and Applied Sciences for Engineering, Faculty of Civil and Industrial Engineering, "Sapienza" University of Rome, Roma, Italy
Email: doretta.vivona@sbai.uniroma1.it, maria.divari@alice.it

Received 29 September 2014; revised 2 November 2014; accepted 16 November 2014

Abstract

In this paper, by axiomatic way, a form of information entropy will be presented on crisp and fuzzy setting. Information entropy is the unavailability of information about a crisp or fuzzy event. It will use measure of information defined without any probability or fuzzy measure: for this reason it is called *general information*.

Keywords

Information, Entropy, Functional Equations, Fuzzy Sets

1. Introduction

The setting of entropy was statistical mechanics: in [1] Shannon introduced entropy of a partition π_A of a set A, linked to a probability measure.

Now, we recall this definition. Let Ω be an abstract space, $\mathcal{A}$ a σ-algebra of subsets A of Ω and P a probability measure defined on $\mathcal{A}$. Moreover $\mathcal{P}$ is the collection of the partition π_A, where

$$\pi_A = \left\{A_1, A_2, \cdots A_n,\ A_i \subset A,\ i = 1,\cdots,n,\ A_i \cap A_j = \varnothing,\ i \neq j,\ \bigcup_{i=1}^n A_i = A\right\}.$$

Basic notions and notations can be found in [2]. Setting $P(A_i) = p_i$ with $\sum_{i=1}^n p_i = 1$ (complete system), Shannon's entropy is

$$H(\pi_A) = H_n(p_1,\cdots,p_n) = -\sum_{i=1}^n p_i \log_2 p_i$$

and it is *measure of uncertainty* of the system π_A. Shannon's entropy is the weight arithmetic mean, where the weights are p_i. Many authors have studied this entropy and its properties, for example: J. Aczél, Daróczy, C. T. Ny; for the bibliography we refer to [3] [4].

How to cite this paper: Divari, M. and Vivona, D. (2014) A Form of Information Entropy. *Natural Science*, **6**, 1282-1285.
http://dx.doi.org/10.4236/ns.2014.617118

Another entropy was introduced by Rényi, called entropy of order α, $\alpha \neq 1$:

$$H_n^\alpha(p_1,\cdots,p_n) = \frac{1}{1-\alpha}\log_2 \sum_{i=1}^n p_i^\alpha,$$

and it was used in many problems [5] [6].

In generalizing Bolzmann-Gibbs statistical mechanics, Tsallis's entropy was introduced [7]:

$$S_n^\alpha(p_1,\cdots,p_n) = \frac{k}{1-\alpha}\left(\sum_{i=1}^n p_i^\alpha - 1\right).$$

We note that all entropies above are defined through a probability measure.

In 1967 J. Kampé de Feriét and B. Forte gave a new definition of information for a crisp event, from axiomatic point of view, without using probability [8]-[10]. Following this theory other authors have presented measures of information for an event [11]. In [12], with Benvenuti we have introduced the measure of information for fuzzy sets [13] [14] without any probability or fuzzy measure.

In this paper we propose a class of measure for the entropy of an information for a crisp or fuzzy event, without using any probability or fuzzy measure.

We think that not using probability measure or fuzzy measure in the definition of entropy of the information of an event, can be an useful generalization in the applications in which probablility is not known.

So, in this note, we use the theory explained by Khinchin in [15] and we give a new definition of entropy of information of an event. In this way it is possible to measure the *unavailability of information*.

The paper is organized as follows. In Section 2 there are some preliminaries about general information for crisp and fuzzy sets. The definitions of entropy and its measure are presented in Section 3. Section 4 is devoted to an application. The conclusion is considered in Section 5.

2. General Information

Let Ω be an abstract space and $\mathcal{C}$ the σ-algebra of crisp sets $C \subset \Omega$. General information J for crisp sets [8] [10] is a mapping

$$J(\cdot): \mathcal{C} \to [0,+\infty]$$

such that $\forall C_1, C_2 \in \mathcal{C}$:

1) $C_1 \subset C_2 \Rightarrow J(C_1) \geq J(C_2)$,
2) $J(\varnothing) = +\infty$, $J(\Omega) = 0$.

In analogous way [12], the definition of measure of general information was introduced by Benvenuti and ourselves for fuzzy sets. Let Ω be an abstract space and $\mathcal{F}$ the σ-algebra of fuzzy sets. General information is a mapping

$$J'(\cdot): \mathcal{F} \to [0,+\infty]$$

such that $\forall F_1, F_2 \in \mathcal{F}$:

1) $F_1 \subset F_2 \Rightarrow J'(F_1) \geq J'(F_2)$,
2) $J'(\varnothing) = +\infty$, $J'(\Omega) = 0$.

3. General Information Entropy

Using general information recalled in Section 2, in this paragraph a new form of information entropy will be introduced, which will be called *general information entropy*. Information entropy means the measure of unavailability of a given information.

3.1. Crisp Setting

In the crisp setting as in Section 2, given information J the following definition is proposed.

Definition 3.1. *General information entropy* for crisp sets is a mapping $E(J(\cdot)): [0,+\infty] \to [0,+\infty]$ with the following properties:

1) monotonicity: $J(C_1) \leq J(C_2) \Rightarrow E(J(C_1)) \geq E(J(C_2))$,
2) universal values: $J(\varnothing) = +\infty \Rightarrow E(J(\varnothing)) = 0$, $J(\Omega) = 0 \Rightarrow E(J(\Omega)) = +\infty$.

The universal values can be considered a consequence of monotonicity.

So, general information entropy $E(\cdot)$ is a monotone, not-increasing function with $E(0)=+\infty$ and $E(+\infty)=0$. Assigned information J on $\mathcal{C}$, the function $E(J(C))=\dfrac{1}{J(C)}$, $C\in\mathcal{C}$ is an example of general information entropy.

It is possible to extend the definition above to fuzzy sets.

3.2. Fuzzy Setting

Given $\Omega, \mathcal{F}, J'$ as in Section 2, the following definition is considered.

Definition 3.2. *General information entropy* for fuzzy sets is a mapping $E'(J'(\cdot)):[0,+\infty]\to[0,+\infty]$ with the following properties:

1) monotonicity: $J'(F_1)\le J'(F_2)\Rightarrow E'(J'(F_1))\ge E'(J'(F_2))$,

2) universal values: $J'(\varnothing)=+\infty\Rightarrow E'(J'(\varnothing))=0,\ J(\Omega)=0\Rightarrow E'(J'(\Omega))=+\infty.$

The universal values can be considered a consequence of monotonicity.

So, general information entropy $E'(\cdot)$ is a monotone, not-increasing function with $E'(0)=+\infty$ and $E'(+\infty)=0.$ Assigned information J' on $\mathcal{F}$ an example of this entropy is $E'(J'(F))=\dfrac{1}{e^{J'(F)}-1}$, $F\in\mathcal{F}$.

4. Application to the Union of Two Disjoint Crisp Sets

In this paragraph, an application of information entropy will be indicated: it concerns the value of information entropy for the union of two disjoint crisp sets. The procedure of solving this problem is the following: first, the presentation of the properties, second the translation of these properties in functional equations, by doing so, it will be possible to solve these systems [16].

It is possible to extend this application also to the union of two disjoint fuzzy sets.

On crisp setting as in Section 2, let C_1 and C_2 two disjoint sets. In order to characterize information entropy of the union, the properties of this operation are used. The approach is axiomatic. The properties used by us are classical $\forall C_1, C_2, C_3, C_1'\in\mathcal{C}$:

(u_1) $J(C_1\cup\varnothing)=J(C_1)$,

(u_2) $C_1'\supset C_1\Rightarrow J(C_1'\cup C_1)\le J(C_1\cup C_1)$,

(u_3) $J(C_1\cup C_2)\le J(C_1)\wedge J(C_1)$ as $C_1\cup C_2\supset C_2$ and $C_1\cup C_2\supset C_2$,

(u_4) $J(C_2\cup C_2)=J(C_2\cup C_1)$,

(u_5) $J((C_1\cup C_2)\cup C_2)=J(C_1\cup(C_2\cup C_3))$.

Information entropy of the union $C_1\cup C_2$ is supposed to be dependent on $E(J(C_1))$ and $E(J(C_2))$

$$E(J(C_1\cup C_2))=\Psi(E(J(C_1)),E(J(C_2))), \tag{1}$$

where $\Psi:[0,+\infty]^2\to[0,+\infty]$.

Setting: $J(C_1)=x$, $J(C_2)=y$, $J(C_3)=z$, $J(C_1')=x'$, with $x, y, z, x', y'\in[0,+\infty]$ the properties $[(u_1)-(u_5)]$ lead to solve the following system of functional equations:

$$\begin{cases} (u_1') & \Psi(x,+\infty)=x, \\ (u_2') & x'\le x\Rightarrow\Psi(x',y)\le\Psi(x,y), \\ (u_3') & \Psi(x,y)\le x\wedge y, \\ (u_4') & \Psi(x,y)=\Psi(y,x), \\ (u_5') & \Psi(\Psi(x,y),z)=\Psi(x,\Psi(y,z)). \end{cases}$$

We are looking for a continuous function Ψ as an universal law with the meaning that the equations and the inequality of the system $[(u_1')-(u_5')]$ must be satisfied for all variables on every abstract space satisfying to all restrictions.

Proposition 4.1. *A class of the solutions of the system* $\left[(u_1')-(u_5')\right]$ *is*

$$\Psi_h(x,y)=h^{-1}\left(h(x)+h(y)\right) \tag{2}$$

where $h:[0,+\infty]\to[0,+\infty]$ *is any continuous bijective and strictly decreasing function with* $h(0)=+\infty$ *and* $h(+\infty)\to 0$.

Proof. The proof is based on the application of the theorem of Cho-Hsing Ling [17] about the representation of associative and commutative function with the right element (here it is $+\infty$) as unit element. □

From (1) and (2) information entropy of the union of two disjoint set is expressed by

$$E\left(J\left(C_1\cup C_2\right)\right)=h^{-1}\left(h\left(E\left(J\left(C_1\right)\right)\right)+h\left(E\left(J\left(C_2\right)\right)\right)\right),$$

where $h:[0,+\infty]\to[0,+\infty]$ is any continuous bijective and strictly decreasing function with $h(0)=+\infty$ and $h(+\infty)\to 0$.

5. Conclusion

By axiomatic way, a new form of information entropy has been introduced using information theory without probability given by J. Kampé De Fériet and Forte. For this measure of information entropy, called by us, general because it doesn't contain any probability or fuzzy measure, it has been given a class of measure for the union of two crisp disjoint sets.

Funding

This research was supported by research center CRITEVAT of "Sapienza" University of Roma and GNFM of MIUR (Italy).

References

[1] Shannon, C. and Weaver, W. (1949) The Mathematical Theory of Communication. University of Illinois Press, Urbana.

[2] Halmos, P.R. (1965) Measure Theory. Van Nostrand Company, New York.

[3] Aczél, J. (2004) Entropies, Characterizations, Applications and Some History. *Proceedings of IPMU*-2004, Perugia, 4-9 July 2004, 1825-1830.

[4] Aczél, J. (1969) Probability and Information Theory. Lectures Notes in Mathematics, 89. Springer-Verlag, Berlin, 1-11.

[5] Rényi, A. (1961) On Measures of Entropy and Information. *Proceedings IV Berkeley Symposium on Mathematical Statistics and Probability*, **1**, 547-561.

[6] Rényi, A. (1970) Probability Theory. Nord Holland/Elsevier, Amsterdam, New York.

[7] Tsallis, C. (1988) Possible Generalization of Bolzmann-Gibbs Statistics. *Journal of Statistical Physics*, **52**, 479-487. http://dx.doi.org/10.1007/BF01016429

[8] Forte, B. (1969) Measures of Information: The General Axiomatic Theory. *RAIRO Informatique Théorique et Applications*, **R3**, 63-90.

[9] Forte, B. (1970) Functional Equations in Generalized Information Theory. In: Cremonese, Ed., *Applications of Functional Equations and Inequalities to Information Theory*, Roma, 113-140.

[10] Kampé de Fériet, J. and Forte, B. (1967) Information et Probabilité. *Comptes Rendus de l'Académie des Sciences Paris*, **265**, 110-114, 142-146, 350-353.

[11] Kampé de Feriét, J. and Benvenuti, P. (1969) Sur une classe d'informations. *Comptes Rendus de l'Académie des Sciences Paris*, **269**, 97-101.

[12] Benvenuti, P., Vivona, D. and Divari, M. (1990) A General Information for Fuzzy Sets. *Uncertainty in Knowledge Bases, Lectures Notes in Computer Sciences*, **521**, 307-316. http://dx.doi.org/10.1007/BFb0028117

[13] Zadeh, L.A. (1965) Fuzzy Sets. *Information and Control*, **8**, 338-353. http://dx.doi.org/10.1016/S0019-9958(65)90241-X

[14] Klir, G.J. and Folger, T.A. (1988) Fuzzy Sets, Uncertainty and Information. Prentice-Hall International Editions, Englewood Cliffs.

[15] Khinchin, A.Y. (1957) Mathematical Foundation of Information Theory. Dover Publications, New York.

[16] Aczél, J. (1966) Lectures on Functional Equations and Their Applications. Academic Press, New York.

[17] Ling, C.H. (1995) Representation of Associative Functions. *Publicationes Mathematicae Debrecen*, **12**, 189-212.

Natural Science, 2014, 6, 1286-1292
Published Online December 2014 in SciRes. http://www.scirp.org/journal/ns
http://dx.doi.org/10.4236/ns.2014.617119

Scientific Research

Using the Resistance Depending on the Magnetic and Electric Susceptibility to Derive the Equation of the Critical Temperature

H. G. I. Hamza[1], M. H. M. Hilo[2], R. Abd Elgani[2], R. Abd Elhai[2], Mubarak Dirar[2]

[1]Department of Physics, Gazera University, Hasahisa, Sudan
[2]Department of Physics, Sudan University of Science and Technology, Khartoum, Sudan
Email: hasabo25@hotmail.com, mhhlo@qu.edu.sa, mahmoud1972@sustech.edu, rawia@sustech.edu, rashaabdelhaye@sustech.edu

Received 23 September 2014; revised 20 October 2014; accepted 15 November 2014

Abstract

In this study the electromagnetic theory and quantum mechanics are utilized to find the resistivity in terms of electric and magnetic susceptibility in which the electron is considered as a wave. Critical temperature of the wire at which the resistance vanishes is found. In this case the resistance being imaginary which leads the real part of the resistance to real zero at critical temperature and the material becomes super conductor in this case. If one considers the motion of electron in the presence of inner magnetic field and resistance force, a new formula for the conductivity is to be found; this formula states that the material under investigation becomes a superconductor at critical temperature and depends on the strength of the magnetic field and friction resistance, and the substance conductivity is found to be super at all temperatures beyond the critical temperature.

Keywords

Susceptibility, Superconductivity, Critical Temperature, Permeability, Permittivity

1. Introduction

In superconductors, the resistance is zero at temperatures less than the critical temperature [1]; in this work, the above concept is proved by taking the conductivity as a function of the permittivity and permeability, and within the existence of the conditions that make the resistance be equal to zero or approach to infinity.

How to cite this paper: Hamza, H.G.I., Hilo, M.H.M., Abd Elgani, R., Abd Elhai, R. and Dirar, M. (2014) Using the Resistance Depending on the Magnetic and Electric Susceptibility to Derive the Equation of the Critical Temperature. *Natural Science*, **6**, 1286-1292. http://dx.doi.org/10.4236/ns.2014.617119

2. Resistivity Formula Due to the Permeability and Permittivity

When the temperature of a conductor approach to the absolute zero, the friction resistance can be ignored [2], if an electron e is induced by an electric field E, then the force on it is given by

$$m\frac{\mathrm{d}v}{\mathrm{d}t} = \mathrm{e}E \tag{1}$$

Including the position variable x in Equation (1) it can be written as

$$m\frac{\mathrm{d}v}{\mathrm{d}x}\frac{\mathrm{d}x}{\mathrm{d}t} = \mathrm{e}E \tag{2}$$

Then

$$\int mv\mathrm{d}v = \int \mathrm{e}E\mathrm{d}x \tag{3}$$

According to the definition of the potential V, we get

$$E = -\frac{\mathrm{d}V}{\mathrm{d}x} \tag{4}$$

From Equation (3)

$$\frac{mv^2}{2} = \mathrm{e}\int\frac{\mathrm{d}V}{\mathrm{d}x}\mathrm{d}x = \mathrm{e}V \tag{5}$$

Then

$$v = \frac{2\mathrm{e}V}{mv} \tag{6}$$

While m is constant, and when the potential difference is constant, then the velocity v is being also constant.

Using Equation (6) and substituting the value of v in the equation of current, that given due to the electron velocity v, charges density n, and the area A, $I = nevA$, then the current I is found to be

$$I = \frac{2Ane^2V}{mv} \tag{7}$$

Then the resistance R is given

$$R = \frac{V}{I} = \frac{V}{nevA} = \frac{Vmv}{Ane[2Ve]} = \frac{mv}{2Ane^2} \tag{8}$$

On other hand R can be written due to the resistivity ρ, the length l, and the crossection area as

$$R = \frac{\rho L}{A} \tag{9}$$

Considering the electron as a wave, its velocity becomes [3]

$$v = \frac{1}{\sqrt{\mu\varepsilon}} \tag{10}$$

Accordingly the resistivity is given by

$$\rho = \frac{m}{2ne^2L\sqrt{\mu\varepsilon}} \tag{11}$$

3. Critical Temperature at a Changing Permeability μ

If a magnetic field with a flux density B, an electric force F_e, besides a friction resistance γv, and a pressure force $\nabla P = \nabla\left(\frac{1}{3}mnv^2\right)$ act together, then the centripetal forces which balance this force is given by [4].

$$\frac{mv_0^2}{r} = Bev_0 + F_e - \gamma v_0 - \frac{m}{3}v_0^2\nabla n \tag{12}$$

where v_0 is the radial velocity, while the friction force and the pressure are given by

$$F_r = \gamma v_0, \quad \nabla P = \frac{1}{3}mv^2\nabla n \tag{13}$$

where γ is the friction coefficient.

$$m\omega_0^2 r = B_0 e\omega_0 r + F_e - \gamma\omega_0 r - \frac{m}{3}\omega_0^2 r^2\nabla n$$

when the outer magnetic field vanishes, then the radial velocity becomes

$$v_0 = \omega_0 r \tag{14}$$

And

$$F_e = m\omega_0^2 r + B_0 e\omega_0 r + \frac{m}{3}\omega_0^2 r^2\nabla n \tag{15}$$

where B_0 denotes the inner magnetic field.

And when an outer magnetic field B is applied, then

$$m\frac{\mathrm{d}v}{\mathrm{d}t} = -\nabla P + F_e + F_r + eB_0 v + Be\,v \tag{16}$$

where F_r is the radial force, and F_m, F_e are the magnetic and the electric forces respectively, which are given by

$$F_B = Bev \quad \text{and} \quad F_e = eE \tag{17}$$

The equation of motion in the presence of the outer magnetic field is given in the form [5].

$$\frac{mv^2}{r} = -\frac{1}{3}mv^2\nabla n + F_e - \gamma v + B_0 e\,v + Be\,v \tag{18}$$

where v is the radial velocity, and while $v = \omega r$ then

$$\begin{aligned} m\omega^2 r &= -\frac{1}{3}m\omega^2 r^2\nabla n + F_e - \gamma\omega r + B_0 e\omega r + Be\omega r \\ &= -\frac{1}{3}m\omega^2 r^2\nabla n + F_e - \gamma\omega r + B_0 e\omega r + Be\omega r + m\omega_0^2 r - B_0 e\omega r + \gamma\omega_0 r + \frac{1}{3}\omega_0^2 r^2\nabla n \end{aligned} \tag{19}$$

when ω is so closed to ω_0 then

$$\omega \to \omega_0 \quad \text{and} \quad \omega + \omega_0 = 2\omega_0$$

$$\omega - \omega_0 = \Delta\omega = \omega_L$$

where ω_L is Larmar frequency, substitute Equation (15) and Equation (19) one gets?

$$m\left(\omega^2 - \omega_0^2\right)r = -\frac{1}{3}m\left(\omega^2 - \omega_0^2\right)r\nabla n - \gamma\left(\omega - \omega_0\right)r + B_0 e\left(\omega - \omega_0\right)r + Be\omega r$$

$$m\left[1 + \frac{r}{3}\nabla n\right]r\left(\omega - \omega_0\right)\left(\omega + \omega_0\right) = -r\gamma\omega_L + B_0 e\omega_L r + Be\omega_0 r$$

$$m\left[1 + \frac{r}{3}\nabla n\right]r\left(2\omega_0\right)\omega_L = -r\gamma\omega_L + B_0 e\omega_L r + Be\omega_0 r$$

Dividing both sides by $\omega_0 r$ we get

$$\left[2m\left[1+\frac{r}{3}\nabla n\right]+\frac{\gamma}{\omega_0}-\frac{B_0 e}{\omega_0}\right]\omega_L = Be \tag{20}$$

$$\omega_L = \frac{e}{\left[2m\left[1+\frac{r}{3}\nabla n\right]+\frac{\gamma}{\omega_0}-\frac{B_0 e}{\omega_0}\right]}B \tag{21a}$$

The current for one atom with Z electrons, moving around its nucleus with a frequency f is

$$i = +Zef = +\frac{Ze}{2\pi}\omega_L \tag{21b}$$

where Z is the atomic number, e is the electron charge, and ω_L is Larmar frequency.

The magnetic torque for one atom is given by

$$M_a = iA \tag{22}$$

where A is the area surrounded by the current which is equal

$$A = \pi r_e^2$$

And from **Figure 1**, one get:

$$x = y = z$$
$$r^2 = x^2 + y^2 + z^2$$
$$r^2 = 3z^2$$
$$\therefore z^2 = \frac{1}{3}r^2$$

But

$$r^2 = z^2 + r_e^2$$
$$\therefore r^2 = \frac{1}{3}r^2 + r_e^2 \tag{23}$$
$$r_e^2 = \frac{2}{3}r^2$$

So the magnetic torque for one atom M_a becomes

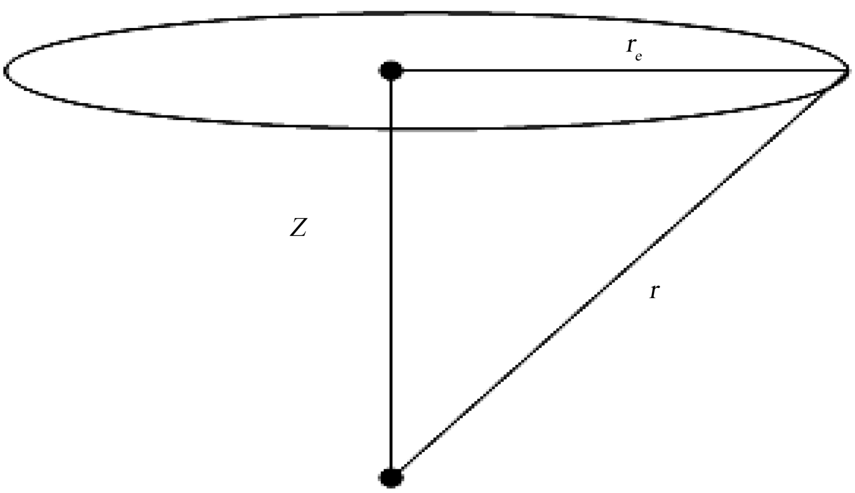

Figure 1. Magnetic torque in *Z* direction.

$$M_a = \frac{2\pi i r^2}{3} \tag{24}$$

If the number of atoms per unit volume is assumed to be N then, the magnetic torque for the matter is

$$M = NM_a = \frac{2\pi}{3} Nr^2 \frac{ze\omega_L}{2\pi} = \frac{Nzer^2}{3}\omega_L \tag{25}$$

$$M = +\frac{Nzer^2\mu_0}{3\left[2m\left[1+\frac{r}{3}\nabla n\right]+\frac{\gamma}{\omega_0}-\frac{B_0 e}{\omega_0}\right]}H \tag{26}$$

According to the definition of susceptibility χ_m then [6].

$$M = \chi_m H \tag{27}$$

Comparing Equations (26) and (27) the susceptibility being

$$\chi_m = +\frac{Nzer^2\mu_0\omega_0}{3\left[2m\left[1+\frac{r}{3}\nabla n\right]\omega_0+\gamma-B_0 e\right]} \tag{28}$$

Then the resistivity in Equation (11) becomes

$$\rho = \frac{m}{2neL\sqrt{\varepsilon_0\mu}} = \frac{m}{2neL\sqrt{\varepsilon_0\mu\frac{Nzer^2\omega_0}{3\left[\frac{2m}{\hbar}\left[1+\frac{r}{3}\nabla n\right]\frac{1}{2}kT+\gamma-B_0 e\right]}}} \tag{29}$$

where $\hbar\omega_0 = \frac{1}{2}kT$ denotes the photon energy.

The resistivity ρ is imaginary, and the real resistivity vanishes when

$$3\left[\frac{2m}{\hbar}\left[1+\frac{r}{3}\nabla n\right]\frac{1}{2}kT+\gamma-B_0 e\right] \le 0$$

$$\text{or}\quad 3\left[\frac{2m}{\hbar}\left[1+\frac{r}{3}\nabla n\right]\frac{1}{2}kT\right] \le B_0 e-\gamma \tag{30}$$

Accordingly the critical temperature becomes

$$T_c = \frac{2\left(B_0 e-\gamma\right)}{3\left[\frac{2m}{\hbar}\left[1+\frac{r}{3}\nabla n\right]\right]k} \tag{31}$$

4. Calculating the Critical Temperature Due to the Conductivity

Assuming that the charges in the conductor are acted by a resistance force F_r, and a magnetic force F_m, besides the electric force F_e, and then the equation of motion becomes [7].

$$F = F_r + F_m + F_e \tag{32}$$

The previous forces are given by the formulas

$$F_0 = k_0 x,\quad F_r = \frac{nmv}{\tau}$$

$$F_m = Bev,\quad F_e = \mathrm{e}E$$

where n, k, x, m, v, e, B, τ and E denotes the density, rigidity coefficient, displacement, mass, velocity, electron charge, magnetic flux density, resolving time, and the electric field respectively.

The equation of motion takes the formula

$$ma = \frac{nmv}{\tau} + Bev + eE \tag{33}$$

When the electron moves with a uniform constant velocity, the Equation (33) becomes

$$\left(\frac{mn}{\tau} - Be\right)v = eE, \quad v = \frac{e}{\left(\frac{mn}{\tau} - Be\right)}E \tag{34}$$

And the conductivity is given by

$$J = n_e ev = \frac{n_e e^2}{\left(\frac{nm}{\tau} - Be\right)}E \tag{35}$$

where n_e the electrons density, while n denotes the density of the medium atoms, accordingly the conductivity being

$$\sigma = \frac{n_e e^2}{\left(\frac{nm}{\tau} - Be\right)}E = \sigma E \tag{36}$$

And the conductivity approaches to infinity when

$$\frac{nm}{\tau} - Be = 0 \tag{37}$$

According to the Maxwell-Boltzmann statistics the density of the atoms in the medium takes the formula [8].

$$n = n_e e^{-\frac{E}{kT}} \approx n_0\left(1 - \frac{E}{kT}\right)$$

Then

$$\frac{mn_0}{\tau}\left(1 - \frac{E}{kT}\right) = Be$$

$$\frac{E}{kT} = 1 - \frac{Be\tau}{mn_0} = \frac{mn_0 - Be\tau}{mn_0}$$

$$T_c = \frac{mn_0 E}{k\left(mn_0 Be\tau\right)} \tag{38}$$

Equation (38) represents the critical temperature in which the conductivity becomes very huge, and when

$$\frac{nm}{\tau} - Be \ll 1 \tag{39}$$

The conductivity also becomes very high, and then

$$\frac{nm}{\tau}\left[1 - \frac{E}{kT}\right] - Be \ll 1 \tag{40}$$

$$1 - \frac{E}{kT} \ll \frac{Be\tau}{mn_0}$$

$$-\frac{E}{kT} \ll \frac{Be\tau}{mn_0} - 1$$

$$\frac{E}{k\left(1-\frac{Be\tau}{mn_0}\right)} \gg T \tag{41}$$

And finally the critical temperature is found to be

$$T_c = \frac{mn_0 E}{k\left(mn_0 - Be\tau\right)} \tag{42}$$

5. Discussion

The classical rules of the electron motion in Equation (1) are used to find the classical formula of the resistivity given in Equation (11), and the electron is considered to be a wave according to the quantum principles and this clarified that the resistivity is a function of the electric and magnetic susceptibility.

The interpretation of Equation (28)—in which we derived the magnetic susceptibility from the electron equation of motion, that depend on the friction force within the friction coefficient γ, the inner magnetic field B_0, the grad of the electrons density ∇n, and the atom radius r—is that when Equation (28) is substituted in Equation (11) the critical temperature at which the resistance vanishes, was found to be in the form that given by Equation (31), which was completely depends on the inner magnetic field B_0, and the friction, within the coefficient γ, the radius r, and the grad of the electron density ∇n.

When we considered the electron motion due to the impact of an inner magnetic field, and a friction resistance, the conductivity was found to be as shown in Equation (36).

The mathematical analysis interprets that the conductivity becomes very high at temperatures less than the critical temperature, which depends on the friction resistance and the inner magnetic field as shown in Equations (41)-(42).

6. Conclusion

The model in which the resistance depends on the electric and magnetic susceptibility, clarifies that the resistance vanishes, and the metal becomes a superconductor at the critical temperature and the temperatures less than it; this relation is not clear in the famous models of the superconductivity.

References

[1] Sales, B.C., *et al.* (2012) Transport, Thermal, and Magnetic Properties of the Narrow Gap Semiconductor $CrSb_2$. *Physical Review B*, **86**, Article ID: 235136. http://dx.doi.org/10.1103/PhysRevB.86.235136

[2] Nguyen, D.N., *et al.* (2009) Temperature Dependence of Total AC Loss in High-Temperature Superconducting Tapes. *IEEE Transactions on Applied Superconductivity*, **19**, 3637-3644.

[3] Slooten, E., *et al.* (2009) Enhancement of Superconductivity near the Ferromagnetic Quantum Critical Point in UCoGe. *Physical Review Letters*, **103**, Article ID: 097003.

[4] Millican, J.N., Phelan, D., Thomas, E.L., Leao, J.B. and Carpenter, E. (2009) *Solid State Communications*, **149**, 707.

[5] Kantorovich, L. (2004) Quantum Theory of the Solid State: An Introduction. Kluwer Academic Publishers, London. http://dx.doi.org/10.1007/978-1-4020-2154-1

[6] Weyeneth, S., Puzniak, R., Mosele, U., Zhigadlo, N.D., Katrych, S., Bukowski, Z., Karpinski, J., Kohout, S., Roos, J. and Keller, H. (2009) Anisotropy of Superconducting Single Crystal $SmFeAsO_{0.8}F_{0.2}$ Studied by Torque Magnetometry. *Journal of Superconductivity and Novel Magnetism*, **22**, 325-329. http://dx.doi.org/10.1007/s10948-008-0413-1

[7] Weyeneth, S., Puzniak, R., Zhigadlo, N.D., Katrych, S., Bukowski, Z., Karpinski, J. and Keller, H.J. (2009) Evidence for Two Distinct Anisotropies in the Oxypnictide Superconductors $SmFeAsO_{0.8}F_{0.2}$ and $NdFeAsO_{0.8}F_{0.2}$. *Journal of Superconductivity and Novel Magnetism*, **22**, 347-351. http://dx.doi.org/10.1007/s10948-009-0445-1

[8] De Visser, A., *et al.* (2009) Muon Spin Rotation and Relaxation in the Superconducting Ferromagnet UCoGe. *Physical Review Letters*, **102**, Article ID: 167003. http://dx.doi.org/10.1103/PhysRevLett.102.167003

Natural Science, 2014, 6, 1293-1295
Published Online December 2014 in SciRes. http://www.scirp.org/journal/ns
http://dx.doi.org/10.4236/ns.2014.617120

Scientific Research

On the Probable Cause of the Discrepancies between Hipparcos and VLBI Pleiades Distance Measurements

Ernst Karl Kunst

Im Spicher Garten 5, Königswinter, Germany
Email: ernstkunst@aol.com

Received 22 September 2014; revised 19 October 2014; accepted 12 November 2014

Abstract

It will show, a recent extension of special relativity on the grounds of a novel concept of velocity, which also predicts the speed of transversal motions on the plane of the sky to increase with enduring observation time, to fully explain the differences of the observational results of the former experiments referring to the distance of the Pleiades from Earth.

Keywords

Pleiades, Discrepancies in Distance Measurements, Duality of Velocity Dependent on One-Way or Two-Way Measurement, Transversal Motions on the Plane of the Sky, Duration of Observation

1. Introduction

It is widely known that the orbiting observatory Hipparcos (High-Precision Parallax Collecting Satellite), launched in 1989 by ESA, among others also measured the distance to the open cluster Pleiades with 118.3 ± 3.5 pc (later publications e.g.: 120.2 ± 1.5 pc), where pc denotes parsec (e.g. [1]). Thereby the satellite measured the apparent position of some well-known cluster stars from different points of Earth's orbit relative to "fixed" distant stars (trigonometric parallax). These measurements covered four years and revealed very small shifts of star positions against the celestial background, being much more precise than ground-based techniques. The latter methods had constantly and correspondingly shown the Pleiades' distance to Earth to be about 133.5 ± 1.2 pc and, thus, to be at odds with the Hipparcos results. Therefore, since the publication of the Hipparcos Catalogue in 1997 this discrepancy has been considered as an unresolved problem.

But very recently a new measurement by using radio interferometry has been published by a cooperation of ten radio telescopes ranging over the whole Earth such that this VLBI (Very Long Base-Line Interferometry)

How to cite this paper: Kunst, E.K. (2014) On the Probable Cause of the Discrepancies between Hipparcos and VLBI Pleiades Distance Measurements. *Natural Science*, **6**, 1293-1295. http://dx.doi.org/10.4236/ns.2014.617120

array acts equivalently to a telescope the size of Earth (e.g. [2]). After a year and a half of observations of four star systems and four stars of the cluster, the network determined a distance of 136.2 ± 1.2 pc; whereby only the far-away quasar J0347+2339 has been used as radio beacon. It is obvious that this result neatly complies with the pre-Hipparcos distance 133.5 ± 1.2 pc, mainly derived by non-trigonometric methods. Therefore, the Hipparcos distance now is widely considered to be in error although according to the authors "no obvious systematic errors seem to be present in the obtained results" [1], *i.e.* the inconsistency between the original Hipparcos and the VLBI distance measurements prevails and the debate regarding the distance to the Pleiades is still open, also since the Hipparcos mission supposedly represents the most complete and exact astrometric survey of the sky and of the Pleiades cluster.

On the other hand, VLBI referenced to an essentially stationary quasar and using the above array of widely separated radio telescopes this gives the resolution of a telescope the size of Earth—as already mentioned. Thus, the latter global telescope essentially simultaneously could observe the apparent motion of oppositely positioned stars of the cluster. Furthermore, one should notice that to derive the cluster's absolute parallax the uncertainties of each target star's position with respect to the center of the cluster have been included, *i.e.* the binary orbit distances have been converted into a single cluster distance or to rephrase this: the apparent motions of the target stars obviously have been referenced to the stationary center of the Pleiades cluster. This implies that all measured apparent motions at opposite positions of Earth's orbit are referenced to the center of the cluster. In contrast to this very special VLBI method, Hipparcos referenced the apparent motion of each target star to some "fixed" star individually such that the measured parallaxes are absolute, *i.e.* the result of a global solution over the whole sky.

2. A Difference of Observation Time of Physical Interest

The above mentioned novel concept of special relativity and the associated modification of the Lorentz transformation among others propose the existence of an absolute rest frame of nature Σ_{oo} in the form of the space-fabric of symmetric Minkowski-space, indicated through the CMB, implying a duality of the speed of light as well as of inertial velocity in dependence on one-way or two-way measurement, respectively [3]. Accordingly will a far-away motion orthogonal to the line of sight with velocity v_0 along length d on the plane of the sky be observed as the vector product of the diverging coordinate differences of space and time, respectively, in the order of

$$\Delta x_{01(v\top)1-\text{way}} = \left|v_0\gamma_0^2\sqrt{\Delta t_d}\right|\cdot\left|\frac{v_0}{c}\left(c\Delta t_{01}\right)\right|\cdot\sin\frac{\pi}{2} = v_0^2\gamma_0^2\sqrt{\Delta t_d}\ , \tag{1}$$

where by angular dimension $\pi/2$ is referred to the angle enclosing the reverse of the vector of the light reaching the observer along the line of sight and d and, furthermore, the angle of the vector of the motion along d relative to the line of sight is running backwards from $\pi/2$ to zero (derivation see [3]). Furthermore, $\Delta t_{01} = 1$, whereas velocity v_0 and Lorentz factor γ_0 denote the respective value relative to the absolute rest frame of nature or the CMB, *i.e.* in this case $v_{o(\text{CMB})} = 370\ \text{km}\cdot\text{s}^{-1}$ of the Sun. In [3] also has been shown that Equation (1) satisfactorily explains the discrepancies between measured and expected values e.g. of the position of the pulsar B1952+32, the running rejuvenation or apparent accelerative behavior of the crab nebula and the measured considerably different time dilations of quasars and supernovae with about the same redshift, *i.e.* distance to Earth. It is clear that Equation (1) must be valid in the case of the Hipparcos and VLBI measurements too, since owing to the Sun's motion relative to the CMB, Earth's orbit projected on the plane of the sky will deliver different, *i.e.* increasing values, in dependence on time of observation. Hence, one convincingly can proceed from the assumption that the discrepancies between the Hipparcos and VLBI measurements also should be due to the relativistic phenomenon expressed through Equation (1).

But from the previous it is obvious that only one of the parallax measurements fulfills the requirements of the coordinate difference of observation time Δt_d in the right-hand square root of Equation (1), that is motion from a point at rest relative to the observer alongside distance d transversal to the latter. With the parallax measurements referenced to the Pleiades center the VLBI time of observation clearly fulfills the above demand. Note that other than VLBI centered at the Pleiades, Hipparcos' four years lasting parallax measurements cover the whole cluster and, thus, also the parallaxes at the opposite sides of Earth's orbit. This implies observation time of VLBI either to be doubled or of Hipparcosless by half, to make both measurements equivalent in the sense of

$\sqrt{\Delta t_d}$ in Equation (1). With this clarification in advance, doubling VLBI observation time one can put the ratio.

$$\frac{\text{Parallax}_{\text{Hipparcos}}}{\text{Parallax}_{\text{VLBI}}} = \left(\frac{\Delta t_{\text{Hipparcos}}}{2 \cdot \Delta t_{\text{VLBI}}}\right)^{\frac{1}{2}} = \frac{\text{distance}_{\text{VLBI}}}{\text{distance}_{\text{Hipparcos}}} \tag{2}$$

of the different distance estimations of both parallax measurements, where Δt in the mid-ratio denotes the respective observation time. This leads in accord with Equation (1) to the further ratio

$$\frac{\text{distance}_{\text{VLBI}}}{\text{distance}_{\text{Hipparcos}}} = \frac{370^2\left(1-\frac{370^2}{c^2}\right)^{-1}\sqrt{4y}}{370^2\left(1-\frac{370^2}{c^2}\right)^{-1}\sqrt{2\times 1.5y}} = 1.1547 \tag{2a}$$

(y in the right-hand ratio denotes year), whereas the respective ratio of the observationally derived VLBI-distance 136.2 ± 1.2 pc and Hipparcos-distance 118.3 ± 3.5 pc delivers:

$$\frac{\text{distance}_{\text{VLBI}}}{\text{distance}_{\text{Hipparcos}}} = \frac{136.2 \pm 1.2\ \text{pc}}{118.3 \pm 3.5\ \text{pc}} = 1.1513 \pm 0.0232\,. \tag{2b}$$

Hence, the latter experimental ratio 1.1513 ± 0.0232 of the above derived distances from measurements of the trigonometric parallax of Earth's orbit at the distance of the Pleiades cluster with differently long observation times seems to be in good accordance with the theoretically derived value 1.1547 of Equation (2a), implying the above discussed discrepancies in distance measurements to owe their existence the relativistic effect Equation (1).

3. Concluding Remarks

The above introduced extension of special relativity [3] seems to fully resolve the discrepancy between Hipparcos and VLBI parallax measurements, additionally to the previously mentioned applications of the former theory. Thus, this additionally shows that physical notions derived from longer lasting observations of motions on the plane of the sky are full of uncertainties and thus either in the reach of the Milky Way Galaxy classical methods or beyond the sphere of the latter redshift measurements alone or in association with luminosity observations must be called upon for sufficiently reliable distance estimations as well.

References

[1] Robichon, N., *et al*. (1999) Open Clusters with Hipparcos. *Astronomy & Astrophysics*, **345**, 471-484.

[2] Melos, C., *et al.* (2014) A VLBI Resolution of the Pleiades Distance Controversy. *Science*, **345**, 1029-1032. http://dx.doi.org/10.1126/science.1256101

[3] Kunst, E.K. (2014) Is the Kinematics of Special Relativity Incomplete? *Natural Science*, **6**, 226-247. http://dx.doi.org/10.4236/ns.2014.64027